1 2 9 0 FACULDADE DE CIÊNCIAS E TECNOLOGIA UNIVERSIDADE D COIMBRA

FATIGUE CRACK GROWTH PREDICTION CONSIDERING CYCLIC PLASTIC STRAIN AND MICRO-VOID MODELLING

E. R. Sérgio[1] • D. M. Neto[1] • F. V. Antunes[1]

[1] CEMMPRE, Department of Mechanical Engineering, University of Coimbra, Portugal

Characterisation of Crack/Notch Tip Fields

6th IJFatigue and FFEMS Joint Workshop

11-13 April 2022
Dubrovnik (Croatia)

Fatigue Crack Growth Mechanisms

- The fatigue crack growth rate is defined by *da/dN*-Δ*K* curves.
- Δ*K* is the crack driving force.
- These curves cannot predict the effect of **stress ratio** or **variable amplitude loading**.

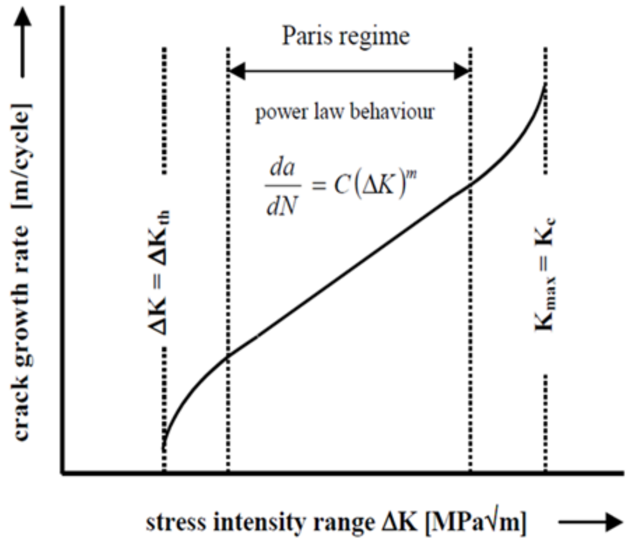

- FCG is due to the occurrence of several, interdependent, **damage mechanisms** at the crack tip zone.

Crack Tip Plastic Deformation

- **Crack tip plastic deformation** is generally assumed to be the main damage mechanism acting at the process zone.
- **Crack closure** has also proved to be a crucial phenomenon in FCG.
- Plastic deformations induce **porous damage:**

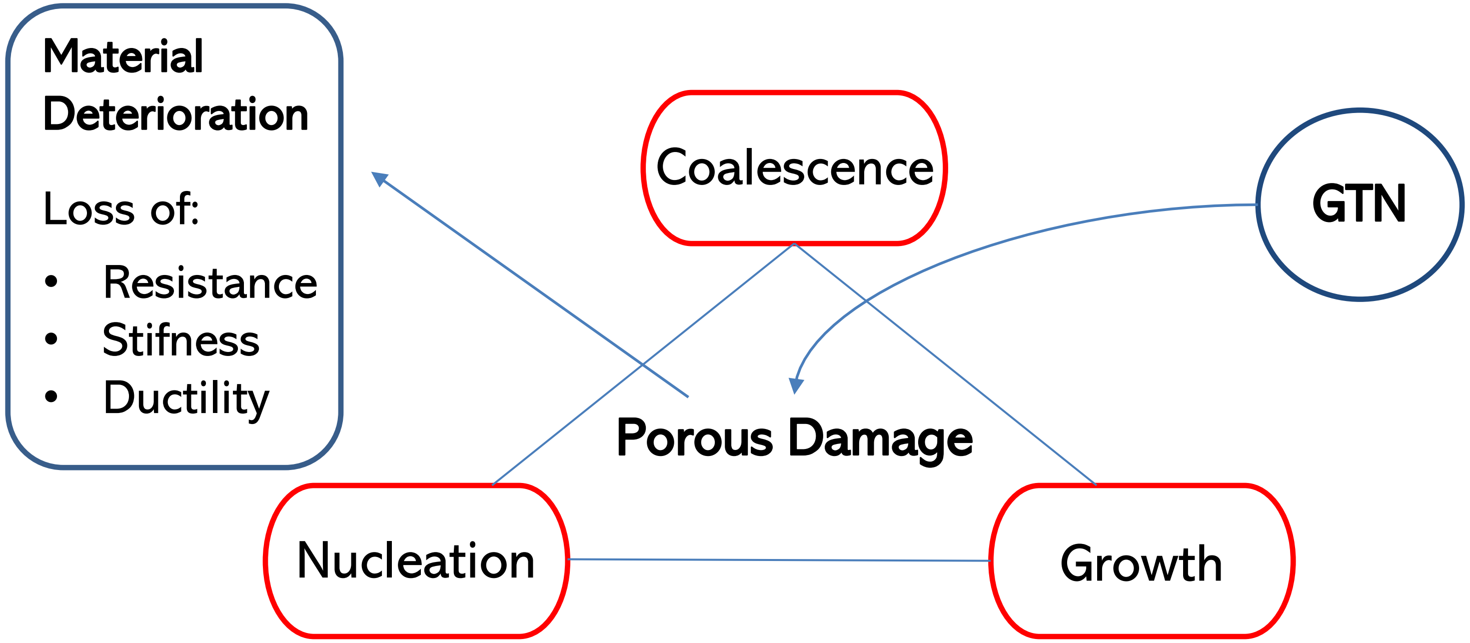

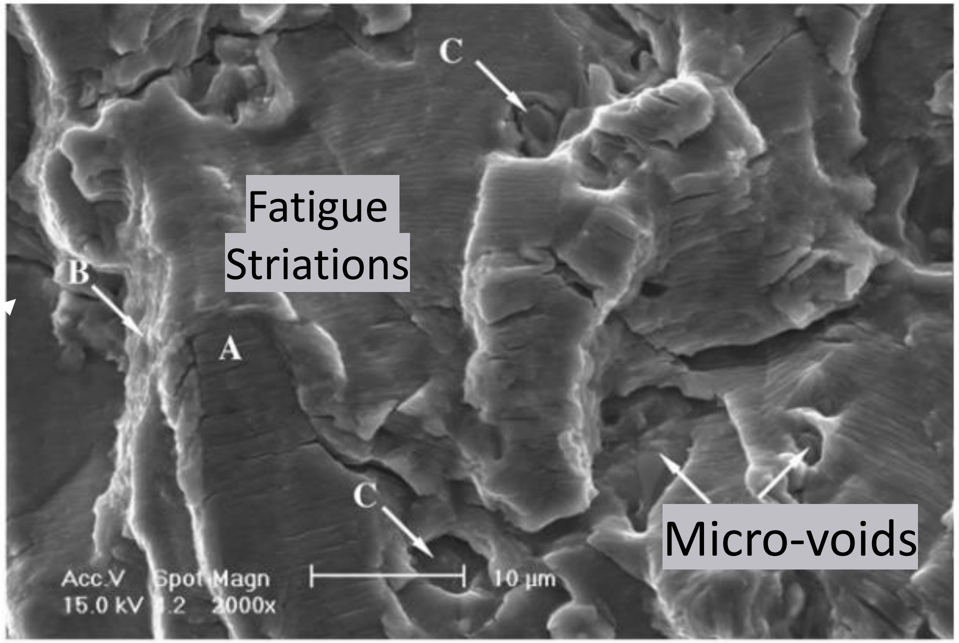

Objectives

- Evaluate the interactions between porous damage, characterized by the **GTN damage**, plastic strain, stress triaxiality and crack closure.

- **Predict** FCG for the 2024-T351 aluminum alloy.

All numerical simulations were performed with the in-house finite element code **DD3Imp**

Material Constitutive Model

- GTN considers a free of voids matrix.
- The shape of the yield surface was defined by the **von Mises** yield criterion.
- The hardening behavior was described by the **Swift** and **Lemaitre–Chaboche** hardening laws.
- The isotropic elastic behavior was given by the generalized **Hooke's law**.

$$\phi = \left(\frac{q^2}{\sigma_y}\right)^2 + 2q_1 f \cosh\left(q_2 \frac{\mathrm{tr}\,\boldsymbol{\sigma}}{2\sigma_y}\right) - 1 - q_3 f^2$$

GTN yield surface

$$\dot{f} = (f - f^2)\dot{\gamma}\sigma_y\, sinh\left(\frac{3p}{2\sigma_y}\right) + \frac{f_N}{s_N\sqrt{2\pi}} exp\left[-\frac{1}{2}\left(\frac{\bar{\varepsilon}^n - \varepsilon_N}{s_N}\right)^2\right]\dot{\bar{\varepsilon}}^p$$

Porosity evolution

$$Y(\bar{\varepsilon}^p) = K\left(\left(\frac{Y_0}{K}\right)^{\frac{1}{n}} + \bar{\varepsilon}^p\right)^n$$

Swift hardening law

$$\dot{\boldsymbol{X}} = C_X\left[\frac{X_{sat}}{\bar{\sigma}}(\boldsymbol{\sigma}' - \boldsymbol{X})\right]\dot{\bar{\epsilon}}_{pl}$$

Lemaitre–Chaboche law

$$E = (1 - f) \cdot E_0$$

Hooke's law considering porosity

Material Parameters

- The **isotropic** and **kinematic hardening parameters** were simultaneously calibrated using the stress–strain curves obtained in smooth specimens of the experimental low cycle fatigue tests.

Elastic properties of 2024-T351 aluminium alloy and parameters for the Swift isotropic hardening law combined with the Armstrong–Frederick kinematic hardening law.

Material	E [GPa]	ν	Y_0 [MPa]	K [MPa]	n	X_{sat} [MPa]	C_X
AA 2024-T351	72.26	0.29	288.96	389.00	0.056	111.84	138.80

- The **GTN parameters**, for this alloy, were obtained from existente literature.

Parameters of the GTN model for the of 2024-T351 aluminium alloy.

Material	f_0	q_1	q_2	q_3	f_N	ε_N	s_N
AA2024-T351	0.007	1.5	1	2.25	0.032	2.25	2.25

Geometry and Discretization

- A compact tension specimen was used in this study. It was loaded, in Mode I, with F_{max}=416.7 N and F_{min}=4.17 N, resulting in a stress ratio, R=0.1.
- The mesh of the specimen considers three distinct zones: a very refined area near the crack tip, a transition zone, and a coarser mesh in the far side of the crack zone.
- 7287 2D **plane strain** finite elements and 7459 nodes were used.

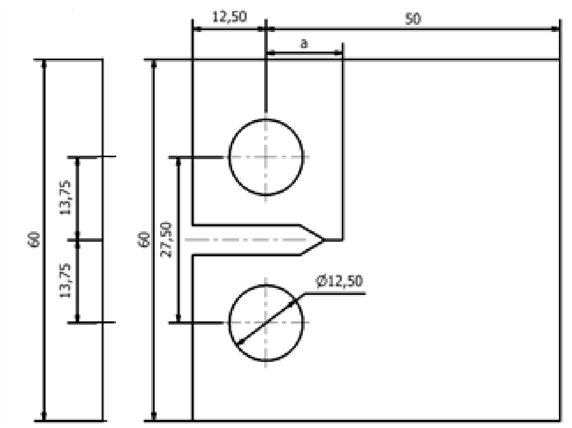

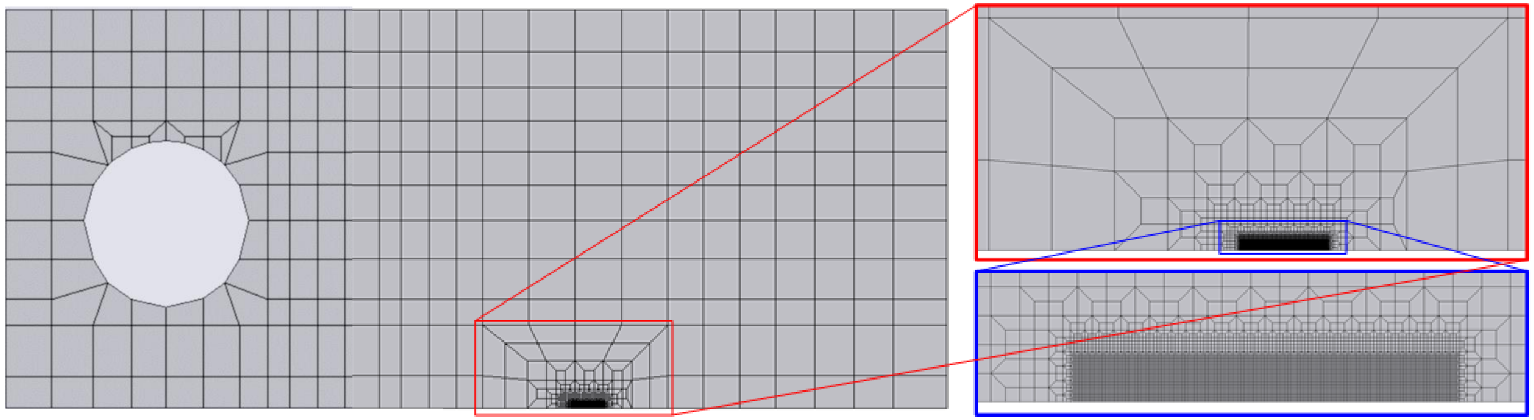

da/dN-ΔK curves

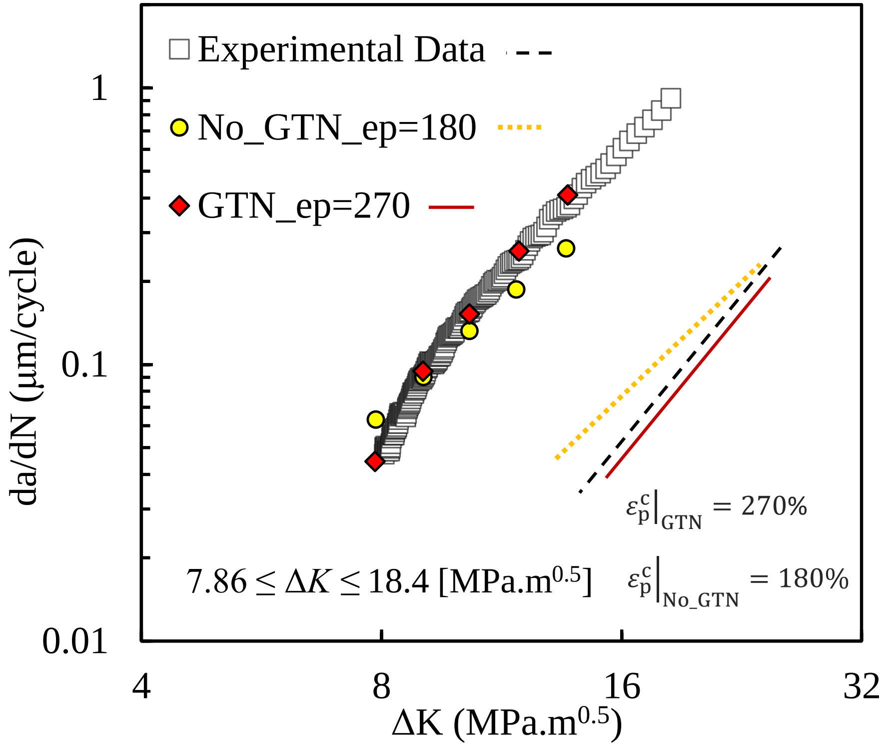

- The results indicate that GTN induces a much **better approximation** to the experimental results.
- As expected, for higher Δ*K* values the GTN model provides **higher FCG rates**.
- However, for lower values of Δ*K*, the GTN model has a **protective behavior**, reducing the *da/dN*.
- This indicates an interrelation between mechanisms at the crack tip.

da/dN-ΔK curves

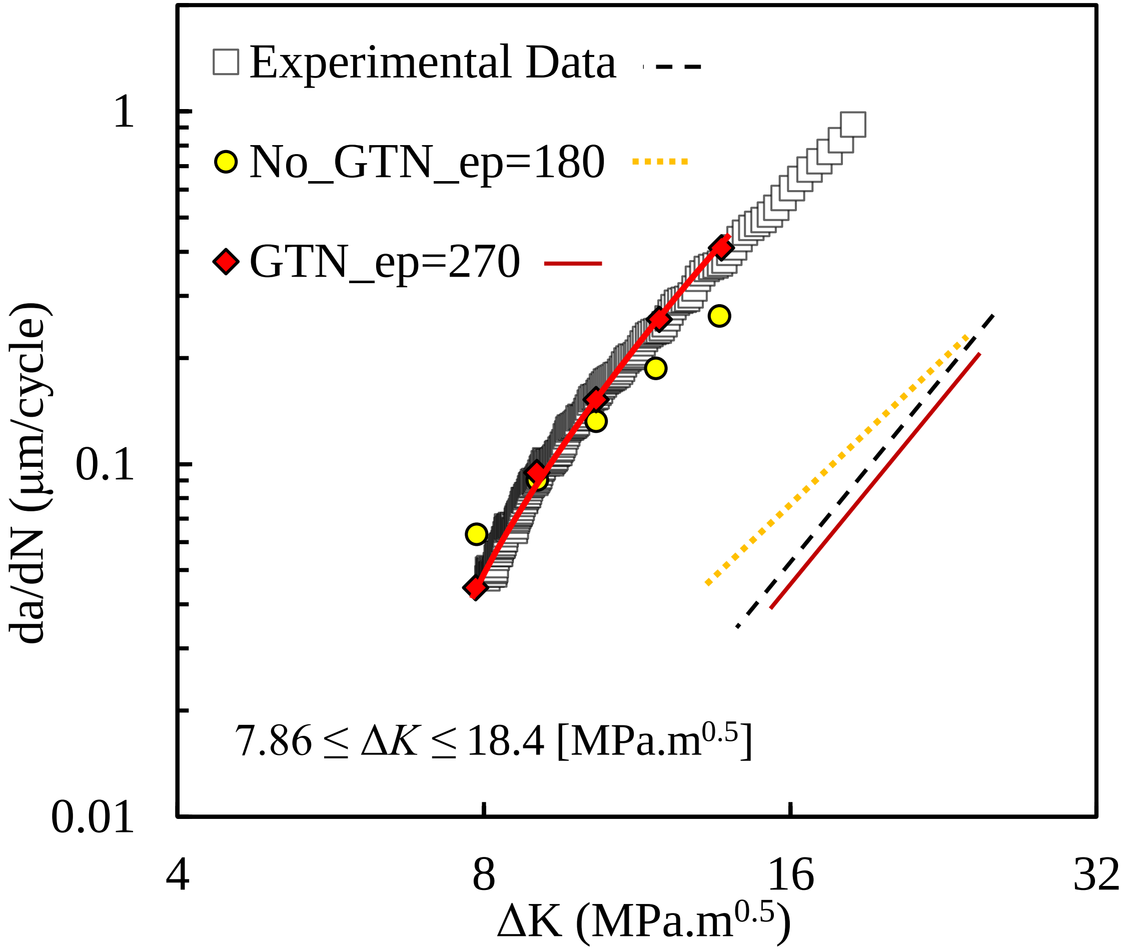

Plastic Strain at the crack tip

- The **plastic strain accumulation** was obtained, on the node containing the crack tip, for two distinct initial crack lengths (a_0):

  - a_0=11.5 mm ($\Delta K = 7.86\ \mathrm{MPa.m}^{-0.5}$) where the model considering GTN predicts a **slower** crack propagation rate.

  - a_0=16.5.5 mm ($\Delta K = 10.36\ \mathrm{MPa.m}^{-0.5}$) where the numerical model considering GTN predicts a **faster** *da/dN.*

- Higher initial crack lengths result in higher Δ*K*'s at stable propagation zone.

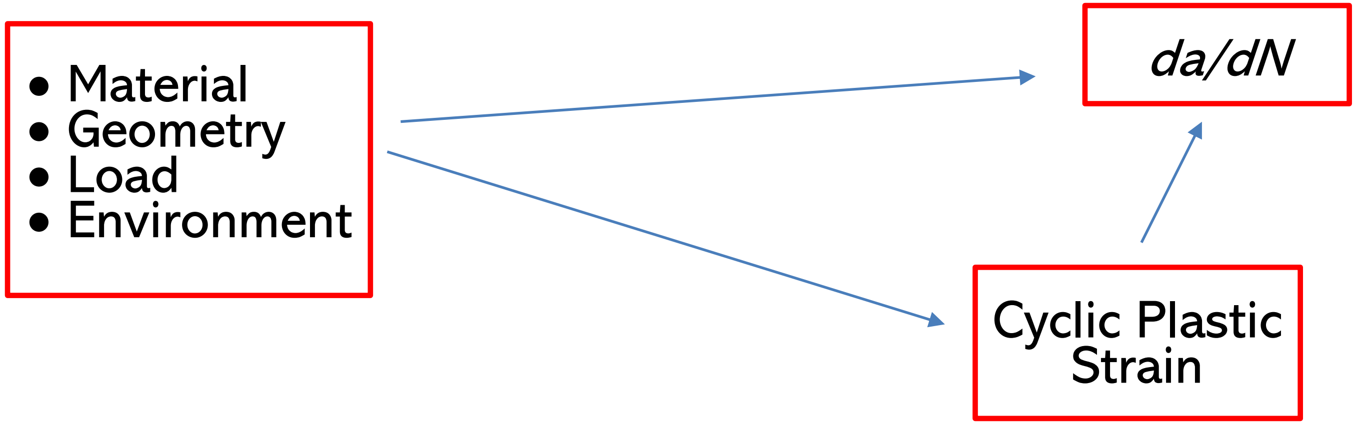

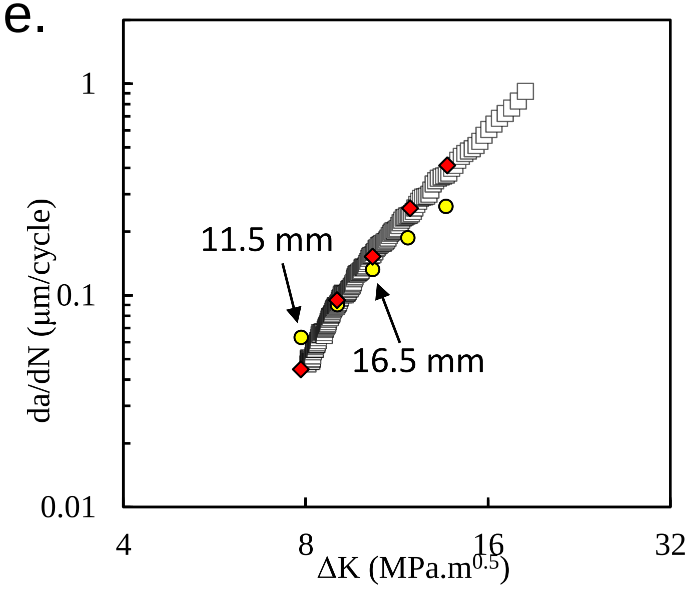

Plastic Strain at the crack tip

- For a_0=11.5 mm the critical plastic strain is achieved faster **without GTN**.
- For a_0=16.5 the **effect of porosity** is such that the critical plastic strain is achieved faster **with GTN**.
- The inversion on the behavior of the plastic strain accumulation evidences the effect of **additional mechanisms** at the crack tip.

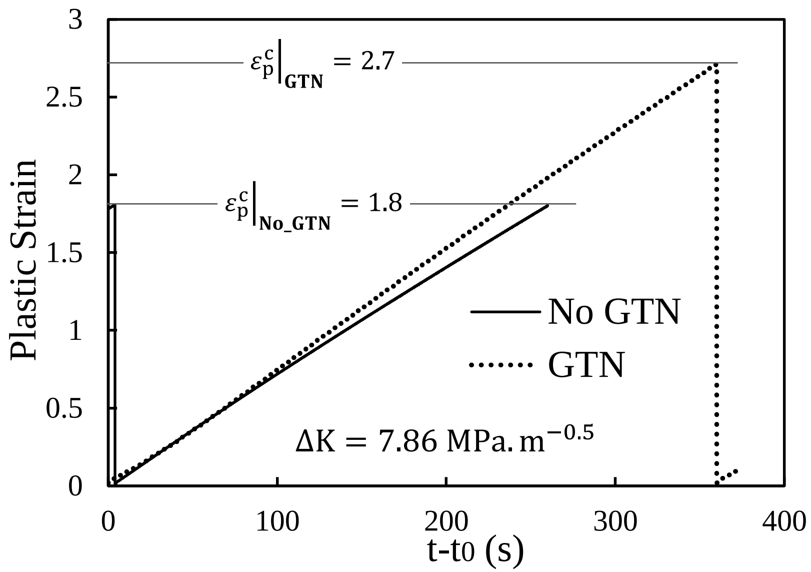

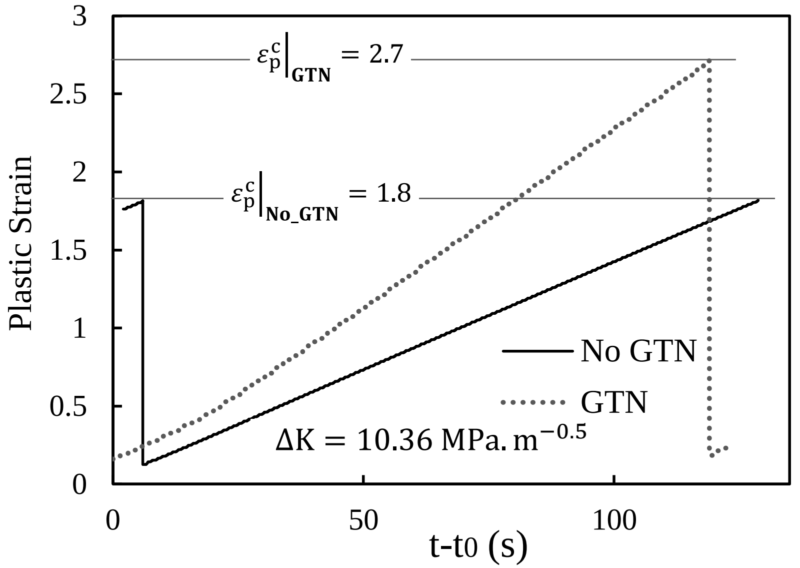

Crack Closure

- For both initial crack sizes the model with GTN **provides higher crack closure levels**.
- By **reducing** the effective intensity of the stress state at the crack tip, it **protects** the material.
- Therefore, crack closure **explains** the *da/dN* results obtained for a_0=11.5 mm.

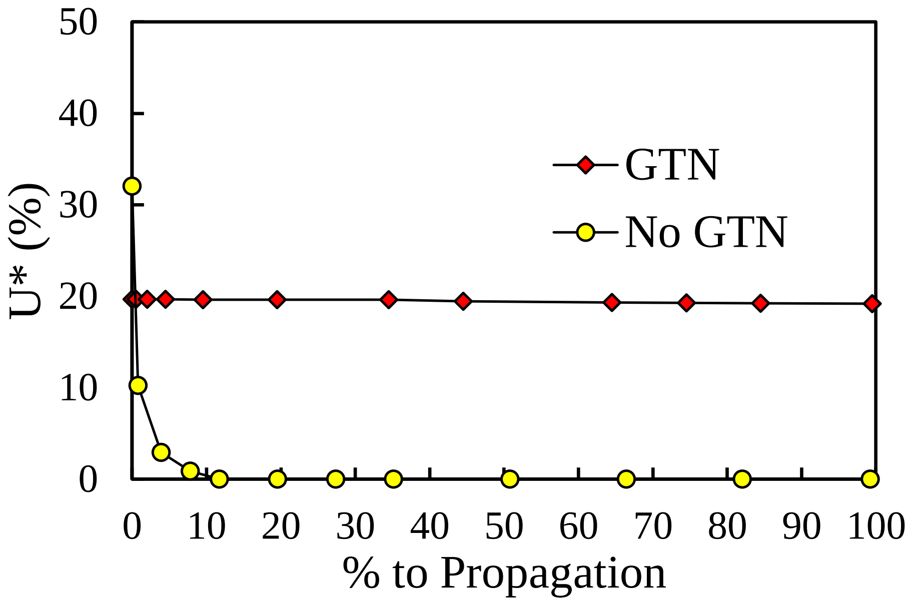

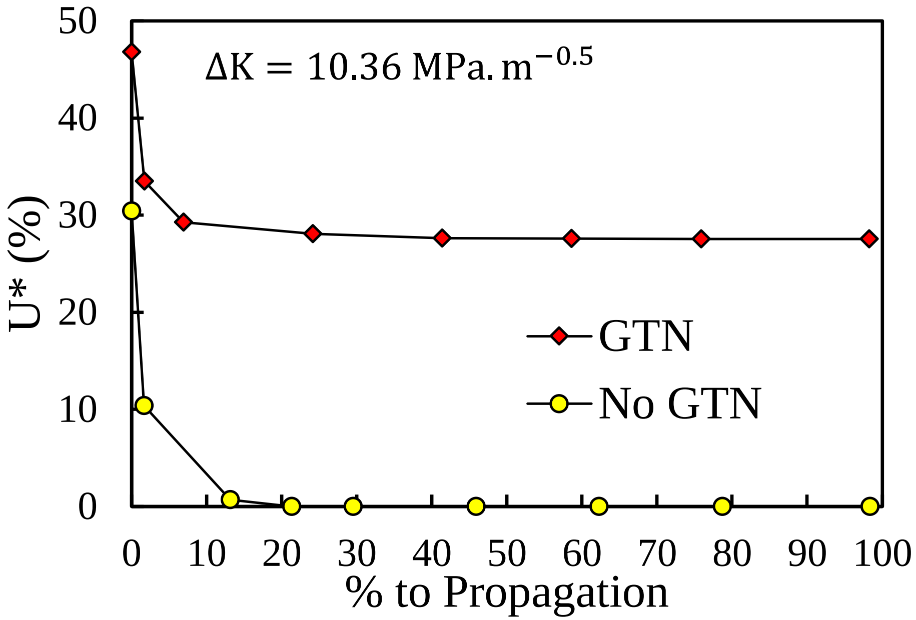

Crack Closure

- Higher crack closure levels occur in the model with GTN because:

  - **The higher plastic strain level stimulates Plastic Induced Crack Closure.**

  - **The inclusion of porosity increases the volume of the deformed material at the crack flanks, increasing the contact between them.**

- For higher ΔK levels, crack closure is not able to fully protect the material. This way, **another mechanism** should rule.

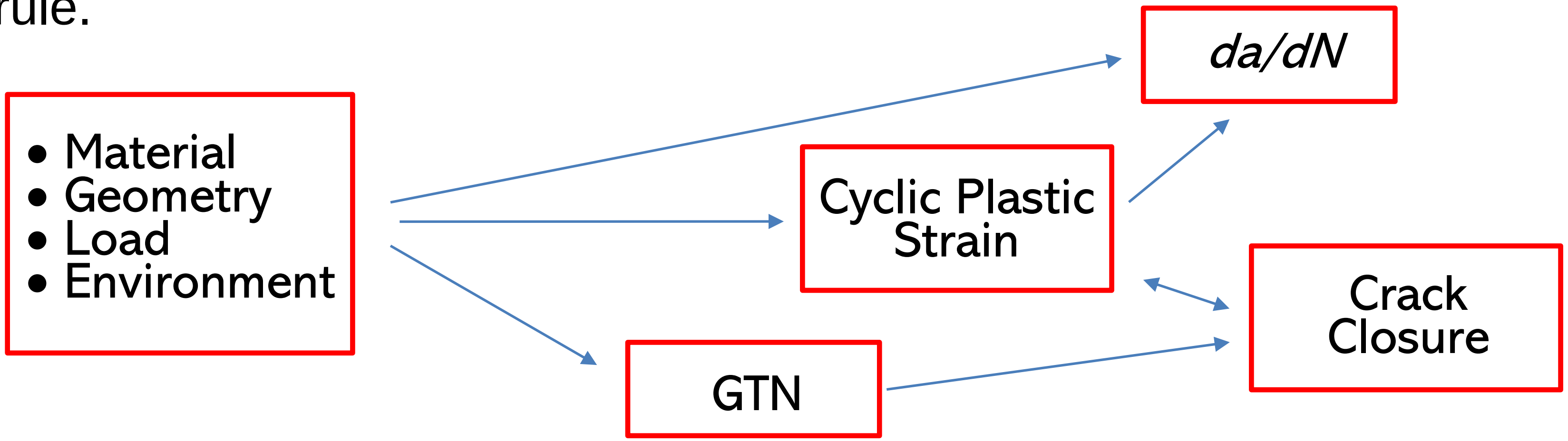

Porosity

- The evolution of the porosity, during a single propagation, was studied for both initial crack lengths.

- For $\Delta K = 7.86\ \mathrm{MPa.m^{-0.5}}$ porosity rises quickly and eventually **saturates**.

Crack Closure Rules

- For $\Delta K = 10.36\ \mathrm{MPa.m^{-0.5}}$ the higher porosity counterbalances the protective effect of crack closure.

Porosity Rules

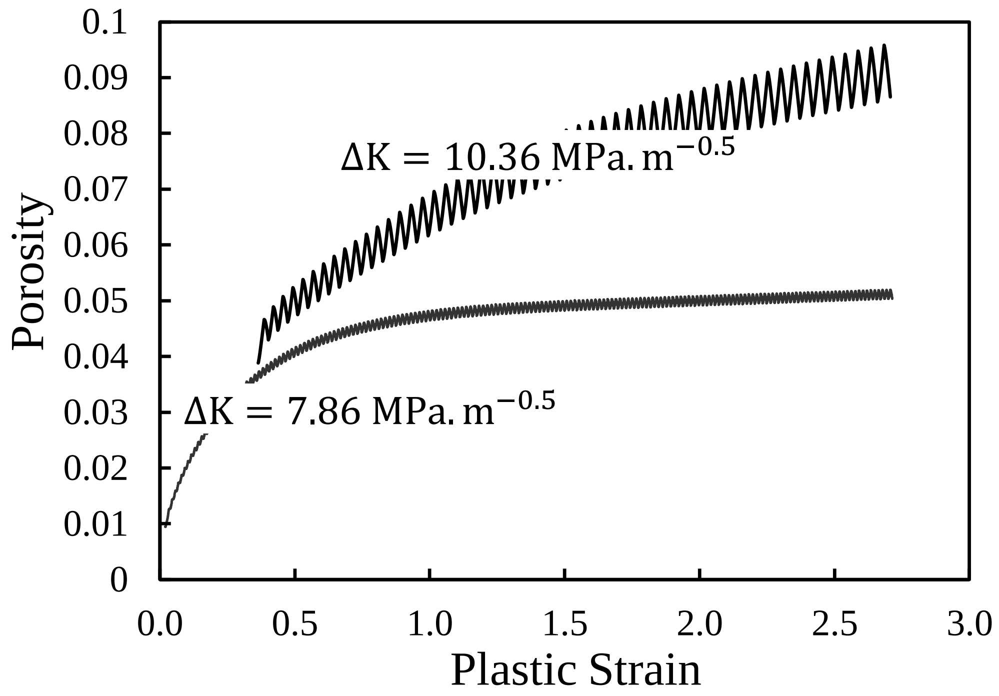

Stress Triaxiality

- The stress triaxiality at the crack tip explains the porosity behaviours.
- The results show na interdepedency of porosity and stress triaxiality.

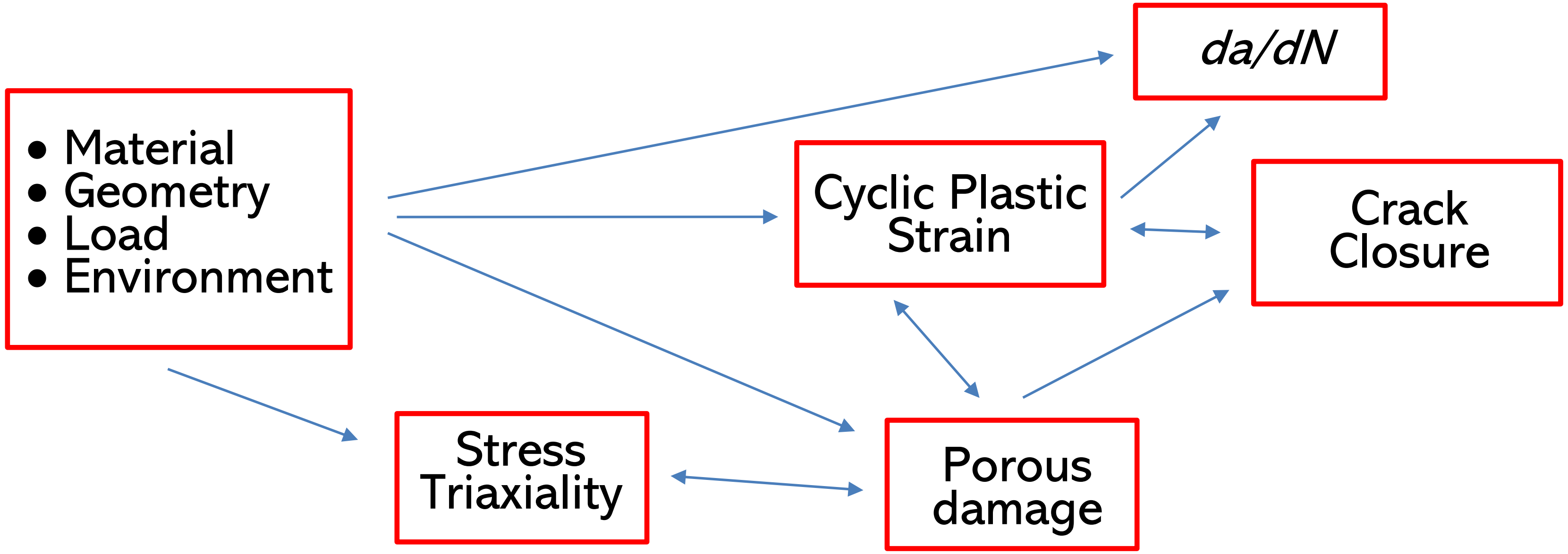

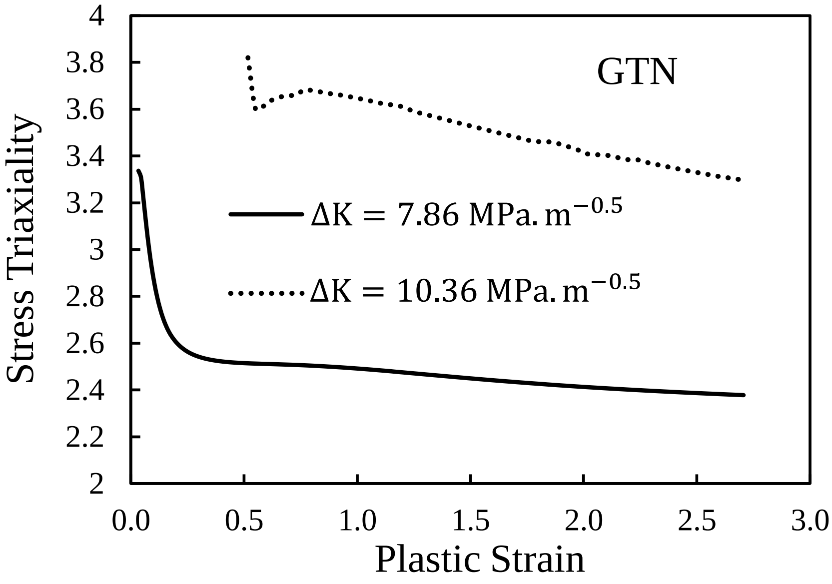

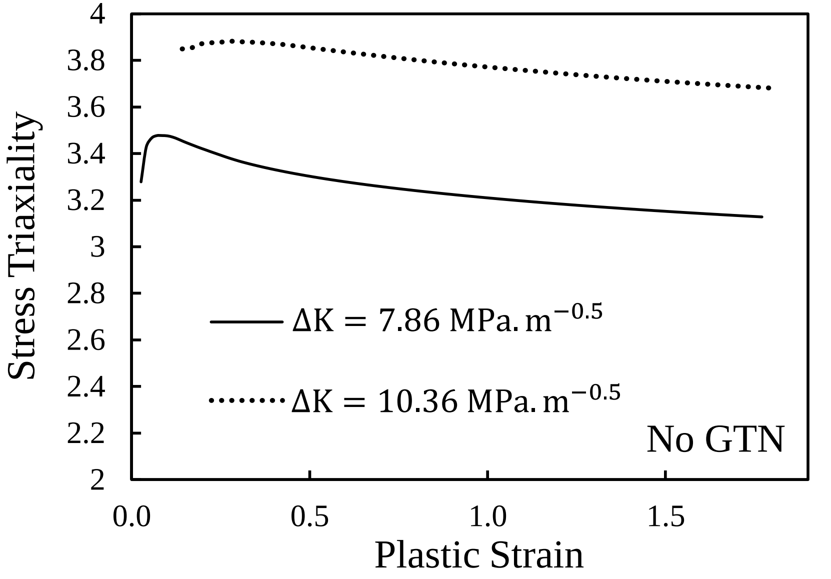

Conclusions

- The GTN version, of the node release numeric model, provides a much **better** approximation to the experimental results.
- **Higher crack closure levels** are generated by higher plastic strain level and crack flank volume.
- Until a certain point crack closure **balances** the porosity effect, then **porosity controls** FCG.
- FCG damage mechanisms should be **analysed as a whole** and not in isolation.

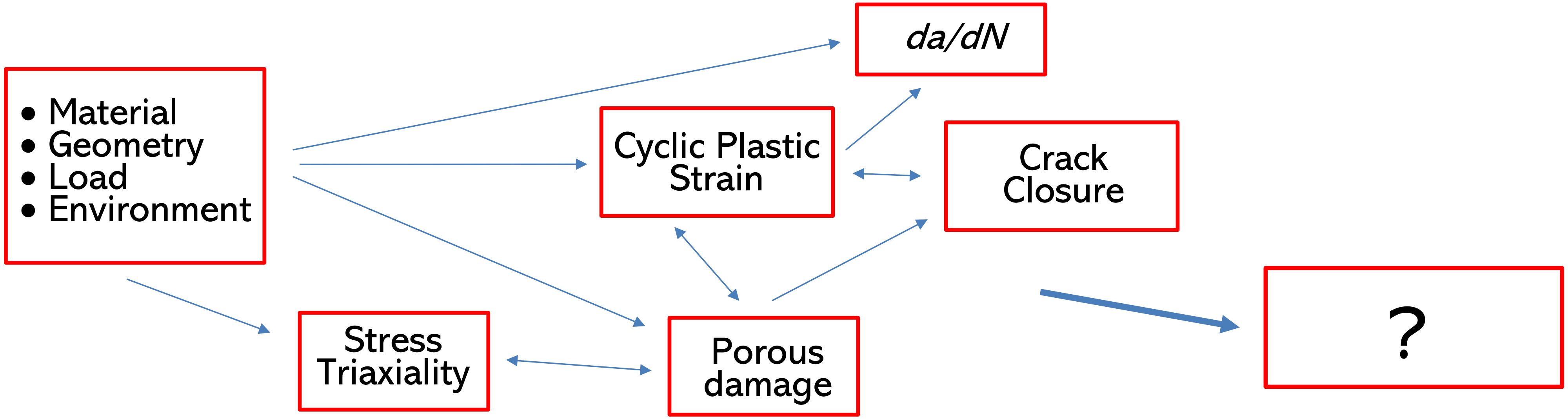

Acknowledgements

This research was funded by Portuguese Foundation for Science and Technology (FCT) under the project with reference PTDC/EME-EME/31657/2017 and by UIDB/00285/2020.

Thank you for your attention!